STRUCTURAL CONTROL AND HEALTH MONITORING
Struct. Control Health Monit. 2016; **23**:1180–1193
Published online 20 January 2016 in Wiley Online Library (wileyonlinelibrary.com). DOI: 10.1002/stc.1838

Mode shape-based damage detection in plate structure without baseline data

Sandris Rucevskis*,†, Rims Janeliukstis, Pavel Akishin and Andris Chate

Institute of Materials and Structures, Riga Technical University, Kalku Street 1, Riga, LV-1658, Latvia

SUMMARY

In this paper, a mode shape curvature-based method for detection and localization of damage in plate-like structures is described. The proposed algorithm requires only the mode shape curvature data of the damaged structure. The damage index is defined as the absolute difference between the measured curvature of the damaged structure and the smoothed polynomial representing the curvature of the healthy structure. To examine the advantages and limitations of the proposed method, several sets of numerical simulations are carried out. Simulated test cases considering different levels of damage severity, measurement noise and sensor sparsity are studied to evaluate the robustness of the method under the noisy experimental data and limited sensor data. Applicability and effectiveness of the proposed damage detection method are further demonstrated experimentally on an aluminium plate containing mill-cut damage. The modal frequencies and the corresponding mode shapes are obtained via finite element models for numerical simulations and by using a scanning laser vibrometer for the experimental study. Copyright © 2016 John Wiley & Sons, Ltd.

Received 3 August 2015; Revised 7 December 2015; Accepted 24 December 2015

KEY WORDS: damage detection; modal analysis; plate; mode shape curvature; structural health monitoring

1. INTRODUCTION

Modern civil, transport and aerospace engineering structures are becoming more complex and multifunctional and are expected to be fully functional under severe environmental conditions. Their failure can lead to tragic consequences, and therefore, structures have to undergo regular costly inspections. Effective non-destructive evaluation techniques for damage detection and structural health monitoring are particularly important for maintaining the integrity and safety of modern engineering structures. Damage identification at the earliest possible stage can increase safety, extend serviceability, reduce maintenance costs, and define reducing operating limits for structures.

In recent years, various vibration-based damage detection methods have been proposed for structural health monitoring. Many of them use various transformations of measured dynamic response of a structure. Dynamic responses, which, in many cases, can be easily obtained, offer damage information, such as the location and severity. These methods are based on the fact that dynamic characteristics, that is, natural frequencies, mode shapes and modal damping, are directly related to the stiffness of the structure. Therefore, changes in these characteristics will indicate a loss of stiffness. Extensive literature reviews of the state of the art in methods for detecting, localizing and characterizing damage by examining changes in the dynamic response of a structure can be found in [1–3]; for example, Qiao *et al.* in [3] compared various damage identification methods for beam-type and plate-type structural elements. These methods were classified into four categories, namely, natural frequency based, mode

*Correspondence to: Sandris Rucevskis, Institute of Materials and Structures, Riga Technical University, Kalku Street 1, Riga, LV-1658, Latvia
†E-mail: sandris.rucevskis@rtu.lv

shape based, curvature of mode shape based and the ones that combine both frequencies and mode shapes. Several advantages and limitations of these methods were also pointed out. Many studies [4–24] confirm that mode shapes and corresponding mode shape curvatures are highly sensitive to damage and can be used for detection and quantification of the damage. Maia *et al.* in [8] performed extensive numerical simulations on a beam structure to compare damage identification sensitivity within different methods, based on the changes of mode shape, mode shape slope, mode shape curvature and mode shape curvature square, respectively. These methods were also tested experimentally on a steel beam with free–free boundary conditions. The authors found that mode shape curvature square method performed better in both numerical and experimental cases. Quiao *et al.* in [9] applied a 2D continuous wavelet transform (CWT) algorithm on numerically simulated mode shapes of a plate with different failure modes. They also compared this method with other techniques, such as 2D gapped smoothing method and 2D strain energy method, and found that 2D CWT outperformed other algorithms in terms of robustness to noise and sensor spacing. Fu *et al.* in [11] exploited a damage identification approach based on local reduction of Young's modulus in a structure by performing numerical simulations of forced vibration response under external force in a cantilevered steel plate. The authors studied single as well as multiple damage scenarios with different levels of noise contamination and measurement point reduction. The researchers concluded that the algorithm is effective and robust for both single and multiple sites of damage. Multiple crack scenarios were also studied by Khiem *et al.* in [12]. The authors derived a simplified expression of natural vibration modes of a beam with an arbitrary number of cracks, which, in combination with a regularization method, allows for estimation of both location and size of multiple cracks. Results indicated that the proposed algorithm was successful at damage identification even at sparse and noisy data conditions. Perez *et al.* in [13] conducted a series of experiments on low-velocity impact damage according to ASTM standards in numerous composite laminated plates. The damage identification procedure consisted of rigorous study of the following damage indicators – frequency shift, mode shape changes and curvature of mode shape changes – all due to damage. The authors concluded that it was hard to make a general conclusion on whether these damage indicators are effectively applicable to all composite structures because the results are highly dependent on the number of measured degrees of freedom and modes. Hammad *et al.* [15] proposed to treat the undamaged zones of the beam as linear elastic, whereas the zones containing multiple cracks are assigned a nonlinear behaviour, thus improving an existing crack model. Results showed that sensitivity of changes in vibration characteristics was proportional to stiffness of a beam support; however, as damage severity increased, the respective change of nonlinearity did not follow the monotonic trend; therefore, it cannot be used for damage detection. Hsu *et al.* [16] suggested a local flexibility method built on a pseudo-local virtual force action on the structure to identify local changes in stiffness in hyperstatic beams. Damage detection studies employed variation of a number of mode shapes. Results showed that only few modes are sufficient in order to identify the damage. Modal strain energy changes in damage identification were exploited by numerous of researchers. Shih *et al.* in [23] showed that damage can be assessed through changes of resonant frequencies, modal flexibility and modal strain energy. The approach was tested on a full-scale slab-on-girder bridge with different damage scenarios. Researchers found that resonant frequency differences were dependent on location and severity of damage; however, Beskhyroun *et al.* in [24] employed operational deflection shapes from the entire frequency range of interest instead of just resonant frequencies. Their studies showed that damage had an influence not only on resonant frequencies but on other frequencies as well and, in some cases, the effect of damage on structure was more pronounced at these other frequencies. In [23], the authors claimed that the location of damage could be found from the peaks in the changes of modal flexibility and modal strain energy. Ooijevaar *et al.* in [17] used a modal strain energy damage index and later standardization of this index according to statistical hypothesis approach, as well as mode shape curvatures, obtained in vibration measurements, to identify impact damage in two advanced skin stiffener composite structures (in 1D and 2D). Results indicated that this method is capable of detecting, localizing and also roughly quantifying the size of barely visible impact damage, although the methodology is affected by the design of the structure and position of the damage and it is crucial to understand the failure mechanisms. Several visual methods are also incorporated in damage detection. Alves *et al.* in [18] proposed a pattern recognition technique to identify the damage – the main features of the undamaged system are set as reference, while the corresponding features of the damaged

DOI: 10.1002/stc

structure are extracted and compared with the reference. Any significant deviation is considered to be a signature of damage. The researchers considered a simply supported steel beam excited with a hammer and shaker with five different damage scenarios. The authors concluded that this algorithm is successful, although the data obtained from impact testing were classified with higher accuracy than that obtained with a shaker. Dworakowski *et al.* in [19] used a digital image correlation to build a deflection curve of a cantilevered beam. After the introduction of damage, these curves were fitted to two line segments, and an angle between segments was taken as a damage index. The authors argued that this methodology utilizes a global damage detection approach using the whole deflection curve at once, therefore giving a noise-free result representation. This approach is capable of detecting small cracks that are not visible to the naked eye. Mosalam *et al.* in [22] used scanning laser stations to visualize and assess the damage of various structures in laboratory conditions, as well as in post-earthquake fields. The researchers justified their approach stating that it is possible to make 3D deformation pattern scans of real objects with high accuracy; post-processing of the obtained graphical images, the method permits a convenient access to the object by scanning from a distance; however, it is possible to acquire data that only form visible surfaces. Dincal *et al.* in [20] proposed a damage detection procedure for beam structures, employing Euler-Bernoulli beam theory. This procedure is based on the assumption that internal stresses in a structure are invariant before and after the application of damage. The damage index was taken as the ratio of the flexural stiffness of the damaged and healthy structure, and it reveals singularities in a curvature profile of a beam structure. The algorithm was validated in an experiment using a cantilevered beam capturing the location, extent and severity of the damage with no significant errors. The same team of authors in [21] attempted to evaluate their own damage identification mechanism [20] by using field measurements – modal data from the Interstate 40 bridge, where four incremental damage sites were introduced via torch cuts in the web and flange of the girder of the bridge. The researchers used the modal flexibility matrix, which was used to approximate the transverse displacements of structure. They argued that each row of the modal flexibility matrix can be interpreted as the deformed shape of a structure because of a unit load applied at the corresponding degree of freedom. Results showed that damage was successfully localized and its severity estimated. In most of these papers, the absolute difference in the mode shape data between the healthy and damaged states of structure is defined as damage index, and the maximum value typically indicates the location of damage. However, the major drawback of these methods is a need for the data of the healthy structure, which sometimes can be difficult or even impossible to obtain. This issue is solved either by using finite element model to simulate the dynamic response of the healthy structure or by employing gapped smoothing techniques [25–27] or smoothing element analysis [28] to generate a smoothed surface of the mode shape curvature obtained from the damaged structure, thus simulating the healthy state of a structure.

In this paper, an ongoing research effort aimed at detecting and localizing damage in plate-like structures by using a mode shape curvature-based method is described. The basic idea of the method is that the mode shape curvature of a healthy structure has a smooth surface and it can be approximated by a polynomial. Using a mode shape curvature data of the damaged structure and a regression analysis with a polynomial approximation, smooth mode shape curvature surfaces of the healthy structure are estimated. The damage index is defined as the absolute difference between the measured curvature of the damage structure and the smoothed polynomial representing the healthy structure, and the maximum value indicates the location and size of the damage. To examine the advantages and limitations of the proposed method, several sets of numerical simulations considering different levels of damage severity, measurement noise and sensor sparsity are carried out. Applicability and effectiveness of the proposed damage detection method are further demonstrated experimentally on an aluminium plate containing mill-cut damage.

2. DAMAGE DETECTION ALGORITHM

The idea of the proposed technique is based on the relationship between the mode shape curvature and the flexural stiffness of a structure. Damage-induced reduction in the flexural stiffness of a structure subsequently causes an increase in the magnitude of the mode shape curvature. The increase in the magnitude of the curvature is local in nature, and thus, it may be considered as an indicator for the

DOI: 10.1002/stc

damage location. Most of the mode shape curvature damage detection methods require the baseline data of the healthy structure for inspection of the change in the modal parameters due to damage. In many cases, such as for structures that are already in service for some time, the baseline modal parameters are rarely available. To overcome this difficulty, a damage index that uses exclusively mode shape curvature data of a damaged structure is proposed.

The basic idea of the method is that the mode shape curvature of the healthy structure has a smooth surface and it can be approximated by a polynomial. Using the mode shape curvature data of the damaged structure and a regression analysis with a polynomial approximation, smooth mode shape curvature surfaces of the healthy structure are estimated. A locally weighted scatter plot smooth using linear least-squares fitting is employed to build the smoothed surface (MATLAB [29]). The local regression smoothing process follows these steps for each datapoint:

1. Compute the *regression weights* for each datapoint in the span. The weights are given by the tricube function:

$$w_i = \left(1 - \left|\frac{x - x_i}{d(x)}\right|^3\right)^3 \tag{1}$$

   where x is the predictor value associated with the response value to be smoothed, x_i are the nearest neighbours of x as defined by the span, and $d(x)$ is the distance along the abscissa from x to the most distant predictor value within the span. The weights have the following characteristics:

   - The datapoint to be smoothed has the largest weight and the most influence on the fit;
   - Datapoints outside the span have zero weight and no influence on the fit.

2. A weighted linear least-squares regression is performed.
3. The smoothed value is given by the weighted regression at the predictor value of interest.

The damage index is defined as the absolute difference between the measured curvature of the damaged structure and the smoothed polynomial representing the healthy structure. The maximum value indicates the location of damage. The damage index generalized to the two-dimensional space for the n^{th} mode at grid point (i,j) is expressed as follows:

$$DI^n_{i,j} = \left|\left(\frac{\partial^2 w^n}{\partial x^2}\right)^2_{(i,j)} - \left(k^n_x\right)^2_{(i,j)}\right| + \left|\left(\frac{\partial^2 w^n}{\partial y^2}\right)^2_{(i,j)} - \left(k^n_y\right)^2_{(i,j)}\right| \tag{2}$$

where w^n is the measured transverse displacement of the structure; k^n_x and k^n_y are smoothed mode shape curvature surfaces in x and y direction, respectively; n is a mode number; and i and j are numbers of grid point in x and y direction, respectively.

The mode shape curvatures are calculated from the mode shapes by the central difference approximation at grid point (i,j) as

$$\left(\frac{\partial^2 w^n}{\partial x^2}\right)_{(i,j)} = \frac{\left(w^n_{i+1,j} - 2w^n_{i,j} + w^n_{i-1,j}\right)}{h^2}, \left(\frac{\partial^2 w^n}{\partial y^2}\right)_{(i,j)} = \frac{\left(w^n_{i,j+1} - 2w^n_{i,j} + w^n_{i,j-1}\right)}{h^2} \tag{3}$$

where h is the distance between two successive nodes or measured points.

In practice, experimentally measured mode shapes are inevitably corrupted by measurement noise causing local perturbations into the mode shape, which can lead to peaks in damage index profiles. These peaks could be mistakenly interpreted as damage, or they could mask the peaks induced by real damage and lead to false or missed detection of damage. To overcome this problem, it is proposed to summarize the results for all modes. The damage index then is defined as the average summation of damage indices for all modes normalized with respect to the largest value of each mode

$$DI_{i,j} = \frac{1}{N}\sum_{n=1}^{N}\frac{DI^n_{i,j}}{DI^n_{\max}} \tag{4}$$

DOI: 10.1002/stc

3. FINITE ELEMENT MODEL AND MODAL ANALYSIS

3.1. Square plate

To evaluate the applicability and effectiveness of the proposed damage detection algorithm, a square aluminium plate 1000×1000 mm of $h = 5$ mm thickness is considered. The elastic material properties are taken as follows: Young's modulus $E = 69$ GPa, Poisson's ratio $v = 0.31$ and the mass density $\rho = 2708$ kg/m^3. Numerical modal analysis is carried out by using the commercial FE software ANSYS (ANSYS, Inc., Canonsburg, Pennsylvania, USA). The finite element model of the plate consists of eight-node shear-deformable shell elements. For the healthy plate, constant flexural stiffness $D = Eh^3/12(1 - v^2)$ is assumed for all elements, while the damaged plate is modelled by reducing the flexural stiffness of the selected elements. Reduction of flexural stiffness is achieved by decreasing the thickness of elements in the damaged region of the plate, thus simulating a cut on one side of the plate. In order to correctly compare the damage detection results, the numerical model is built according to the experimental setup. The plate is divided into 52×52 elements, and the clamped boundary conditions are applied at all four edges of the plate. The mode shapes are extracted from 51×51 nodes in the region $20 \leq x \leq 980$ and $20 \leq y \leq 980$ of the plate; thus, boundary nodes at all four edges of the plate are excluded from the damage detection analysis. The modal frequencies and corresponding mode shapes for 12 modes are extracted from all 51×51 nodes in the damaged plate model.

Several sets of simulated data are used to investigate the effectiveness of the proposed algorithm for damage detection in plate-like structures. Five different levels of damage severity (cut depth) are introduced in the region $270 \leq x \leq 350$ and $640 \leq y \leq 700$ representing 0.48 % of the plate area (Figure 1). Cut depths of $h_1 = 0.5$, 1, 1.5, 2 and 2.5 mm are assumed.

To ascertain the sensitivity of the proposed algorithm to noisy experimental data, a series of uniformly distributed random variables is added to the numerical mode shapes to generate the noise-contaminated mode shapes

$$w^n = \widetilde{w}^n(1 + \delta(2r - 1)) \tag{5}$$

where $\widetilde{w}^n$ is noise-free transverse displacement of the structure, r is the uniformly distributed random values in the interval $(0, 1)$ and δ is the noise level. In this study, four different noise levels $\delta = 1 \times 10^{-2}$, 5×10^{-3}, 1×10^{-3} and 5×10^{-4} are examined. Combination of different noise levels and cut depths results in 20 simulated test cases, which are given in Table 1.

Although the latest measurement systems such as scanning laser vibrometer (SLV) allow obtaining high-density mode shape data, in practice, mode shapes often can be only measured using relatively sparse distribution of sensors, and thus, the robustness of the proposed method under limited datapoints is of interest. In order to evaluate the effect of different number of measured mode shape datapoints on the performance of the method, it is proposed to divide the initial matrix of 51×51 datapoints by integer values of $p = 1$, 2, 3, 4 and 5. In these five cases, the extracted mode shape data form the following matrices: 51×51, 26×26, 17×17, 13×13 and 11×11. For comparison purposes, the cut depth of 2 mm and the noise level $\delta = 2 \times 10^{-3}$ are assumed.

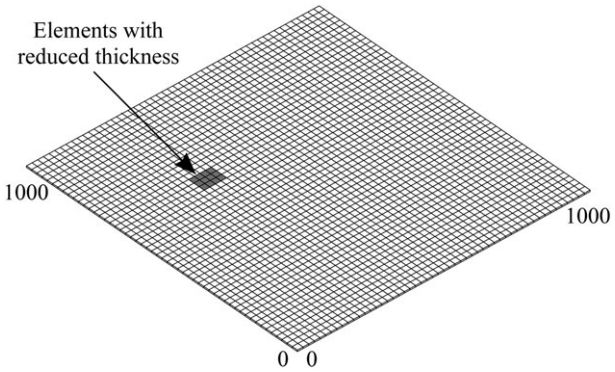

Figure 1. Finite element model for a square plate with an area of reduced stiffness.

DOI: 10.1002/stc

Table I. Calculated false-positive damage indication ratios for the simulated test cases.

	Noise level $\delta = 1 \times 10^{-2}$			Noise level $\delta = 5 \times 10^{-3}$			Noise level $\delta = 1 \times 10^{-3}$			Noise level $\delta = 5 \times 10^{-4}$		
Confidence level Cut depth [mm]	90%	95%	99%	90%	95%	99%	90%	95%	99%	90%	95%	99%
0.5	—	—	—	—	—	—	1.42	0.12	0	0.66	0.04	0
1.0	—	—	—	7.83	1.79	0.08	1.33	0.21	0	0.25	0	0
1.5	—	—	—	7.08	1.67	0.04	0.96	0.08	0	0	0	0
2.0	8.29	1.58	0.04	6.50	1.25	0.04	0.62	0.04	0	0	0	0
2.5	7.91	2.17	0.21	5.66	0.87	0.04	0.12	0	0	0	0	0

3.2. Rectangular plate

In order to evaluate the robustness of the proposed algorithm to different aspect ratios of the plate, a rectangular aluminium plate 1000×400 mm of $h = 5$ mm thickness with the same physical properties as the square plate is also examined. The plate is divided into 52×22 elements, and the clamped boundary conditions are applied at all four edges of the plate. The mode shapes are extracted from 51×21 nodes in the region $20 \leq x \leq 980$ and $20 \leq y \leq 380$ of the plate. Mill-cut damage with a depth of 2 mm is introduced in the region $270 \leq x \leq 350$ and $240 \leq y \leq 270$ of the plate. In total, 12 modal frequencies and corresponding mode shapes are calculated. The noise level $\delta = 2 \times 10^{-3}$ is added to the calculated mode shapes to generate the noise-contaminated mode shapes.

4. EXPERIMENTAL SETUP

For the experimental validation of the proposed damage detection algorithm, an aluminium plate with the same physical and geometrical properties as for the numerical study is considered. Mill-cut damage with a depth of 2 mm is introduced in the region $270 \leq x \leq 350$ and $640 \leq y \leq 700$ of the plate. The clamped boundary conditions are realized by fixing the plate into a specially designed aluminium frame (Figure 2). The distance of 18 mm of each edge of the plate is fixed between the frame and the solid aluminium bar, which are tied together by means of bolts with the spacing distance of 100 mm. The clamping strength is realized by applying 20 Nm of fastening torque onto the bolts. To ensure uniform pressure through the whole contact surface, an aluminium beam with the same

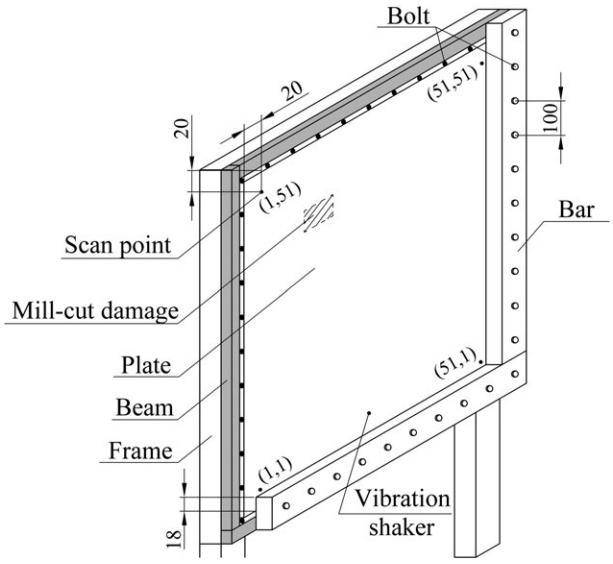

Figure 2. Experimental setup of the test plate.

DOI: 10.1002/stc

thickness and physical properties as the test plate is inserted between the frame and the bar on the other side of the bolts.

The resonant frequencies and corresponding mode shapes of the plate are measured by a POLYTEC PSV-400-B scanning laser vibrometer. General experiment setup consists of a PSV-I-400 LR optical scanning head equipped with a highly sensitive vibrometer sensor (OFV-505), OFV-5000 controller, PSV-E-400 junction box, a Bruel & Kjaer type 2732 amplifier and a computer system with a data acquisition board and PSV software. The scanning grid of 51×51 measurement points with the first measurement point located at the distance of 20 mm from each edge of the plate is defined. The plate is excited by a periodic input chirp signal generated by the internal generator with an 800-Hz bandwidth through a vibration shaker. After the frequency response function and resonant frequencies are obtained, the plate is excited by a periodic sine wave signal with correspondence to each resonant frequency in order to obtain the corresponding mode shape. When the measurement is performed in one point, the vibrometer automatically moves the laser beam to another point of the scan grid, measures the response using the Doppler principle and validates the measurement with the signal-to-noise ratio. The procedure is repeated until all scan points have been measured. The mode shapes are obtained by taking the fast Fourier transform of the response signal. In total, 12 mode shapes are measured.

5. RESULTS OF DAMAGE DETECTION

For the illustration of the proposed damage detection algorithm, the general workflow implemented in MATLAB is given as follows:

1. For the numerical test case, a finite element model with the selected cut depth is built, and the modal frequencies and corresponding mode shapes are extracted from all 51×51 nodes. For each of $n = 1, \ldots, N$ modes, a two-dimensional array of transverse displacements $\widetilde{w}^n_{i,j} = \widetilde{w}^n\left(x_i, y_j\right), (1 \leqslant i,j \leqslant I), I = 51$ is formed. For the experimental test case, transverse displacements $w^n_{i,j} = w^n\left(x_i, y_j\right), (1 \leqslant i,j \leqslant 51)$ are recorded by means of laser vibrometer, and similarly, a two-dimensional array is formed.
2. In the next step for each mode, the noise level δ is assigned to calculated mode shapes to generate noise-contaminated mode shapes $w^n_{i,j}$ according to Eqn (5).
3. From the recorded quantities $w^n_{i,j}$, second-order derivatives $(\partial^2 w^n/\partial x^2)_{ij}, (\partial^2 w^n/\partial y^2)_{ij}$ are calculated by the central difference approximation (Eqn (3)) for each $i,j = 2, \ldots, I-1$.
4. The smoothed mode shape curvature surfaces k^n_x and k^n_y are estimated by using the calculated second-order derivatives and the weighted linear least-squares regression with a second-degree polynomial approximation. It should be noted that the smoothing process is considered local because each smoothed value is determined by neighbouring datapoints defined within the span. In this study, the span is defined by 10% of the total number of datapoints in order to fit the original surface as close as possible and not to smooth out too much information. The selection of the span is especially important because of possible quick changes of sign of neighbouring mode shape curvature values when the higher modes and a sparse distribution of sensors are considered (Figure 3).
5. Damage indices $DI^n_{i,j}$ are calculated according to Eqn (2). The absolute difference between the measured curvature and the smoothed polynomial in x and y directions is normalized with respect to the largest value of the respective component so that both components have equal weight in calculating damage index.
6. Finally, damage indices $DI_{i,j}$ for all modes are estimated by Eqn (4).

Smoothing process of the mode shape curvature of the damaged structure is the most important part of the proposed method for its successful application; therefore, illustration of the process is given in Figures 3 and 4. Mode shape of the highest experimentally measured mode (in terms of both natural frequency and nodal lines [4, 4]) of the plate and the corresponding second-order derivatives in x direction are presented in Figure 4. In this case, a matrix of 17×17 measured datapoints is employed to build the mode shape and calculate the derivatives. The importance of the span selection for the

DOI: 10.1002/stc

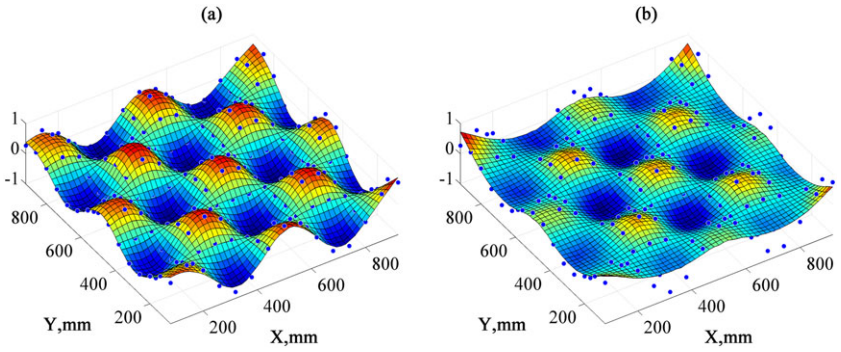

Figure 3. The smoothed surface of the mode shape curvature in x direction: (a) span – 10% of the total number of datapoints and (b) span – 25%.

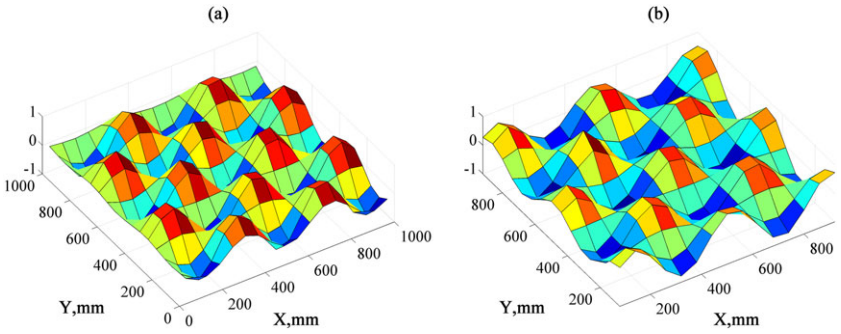

Figure 4. The 12th mode of the test plate: (a) mode shape and (b) mode shape curvature in x direction.

surface smoothing is illustrated by two examples (Figure 3): in the first case, the span is defined by 10% of the total number of datapoints and, in the second one, by 25%. It can be noticed that in the first case, the smoothed surface (surface plot) fits most of the initial datapoints (blue standalone points), and therefore, the largest absolute differences (used for calculation of damage indices) in measured curvature and smoothed surface are to be expected because of damage and subsequently could point at the damage location. On the other hand, when 25% of datapoints are used for span definition, the smoothed surface still represents the pattern of the curvature like for the 10% case, but most of the initial datapoints fall off the surface. In this case, the absolute difference between the calculated and smoothed surfaces will result in noisier damage index plot and thus is much less useful for damage detection.

Damage detection results according to Eqn (4) for the experimental test case and the corresponding simulated test case (cut depth – 2 mm, noise level $\delta = 2 \times 10^{-3}$) using original matrix of 51×51 datapoints are given in Figure 5. Although in both cases, the peak values occur at the predetermined

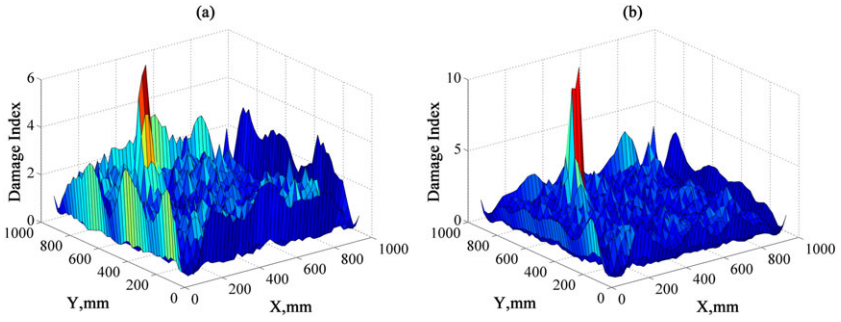

Figure 5. Damage indices DI_{ij} for (a) the experimental and (b) simulated test cases.

DOI: 10.1002/stc

damage location, it can be seen that large values also emerge at the boundaries of the plate and some smaller peaks are present at other areas of the plate where no damage has been introduced.

The boundary distortion problem is caused by discontinuity of mode shapes at their ends because of clamped boundary conditions. In some cases, those extreme values can mask the peaks induced by real damage and lead to false or missed detection of damage. There are two commonly used methods to reduce the boundary effect [9]. One method is to extend the mode shape data beyond the original boundary by the cubic spline extrapolation based on the points near the boundaries. The other method is simply to ignore those values near the boundaries by cutting them off or setting them to zero. In this study, the latter method is adapted. It should be noted that neither the extrapolation method nor the 'set-to-zero' method is capable of detecting damage close to the boundaries, because both of them smooth out the information near the boundaries.

To deal with the problem of other smaller peaks, the concept of the statistical hypothesis testing technique [30] is used. For this reason, the damage indices determined for each node are standardized, and the concept of the statistical hypothesis testing is used to classify damaged and undamaged elements and to localize damage depending on the predefined damage threshold value. The standardized damage index Z_{ij} at grid point (i,j) is obtained as follows:

$$Z_{ij} = \frac{DI_{ij} - \mu_{DI}}{\sigma_{DI}} \tag{6}$$

where μ_{DI} and σ_{DI} are the mean value and standard deviation of the damage indices, respectively. The decision on the localization of damage is established based on the level of significance used in the hypothesis test, which can be determined from a pre-assigned classification criterion. The typical damage threshold values for the standardized damage index widely used in literature include 1.28, 2 and 3 for 90%, 95% and 99% confidence levels for the presence of damage.

To classify the damaged elements, it is proposed to truncate the values of damage indices smaller than three units according to the standardized damage index threshold value for the 99% confidence level for the presence of damage. Now, the damage detection results for both cases clearly reveal the predetermined damage location as shown in Figure 6. Similarly, the damaged elements are classified for the other two confidence levels (Figures 7 and 8). It can be seen that in general, for both cases, damage indices clearly point at the predetermined damage location; however, other insignificant peaks have passed the pre-assigned damage index threshold for both the 90 and 95% confidence levels and can be classified as damage. On the other hand, it must be noted that only five out of 12 employed mode shapes for the experimental test case and six out of 12 for the simulated test case are affected by the introduced damage and their corresponding damage indices could individually point the damage location.

To analyse the influence of the noise level and damage severity on the effectiveness of the proposed method, a false-positive damage indication ratio R is introduced. False-positive indication of damage means that standardized damage indices outside the predetermined damage location have passed the pre-assigned damage classification criterion and indicate the presence of damage although no damage is introduced there. The ratio represents the relationship between a number of nodes with a false-positive damage indication and the total number of nodes for the plate:

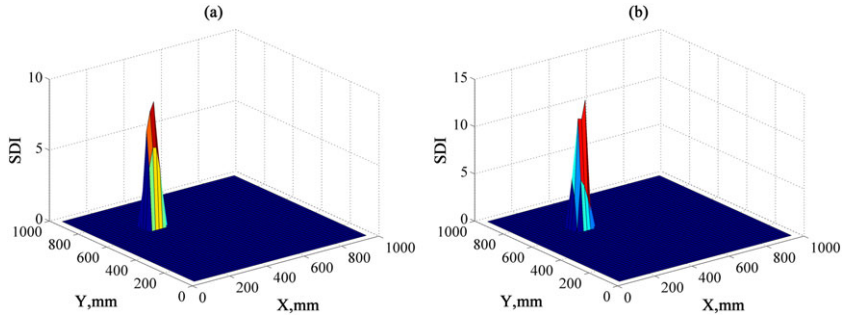

Figure 6. Standardized damage indices (SDIs) Z_{ij} for (a) the experimental and (b) simulated test cases after truncation according to the 99% confidence level.

DOI: 10.1002/stc

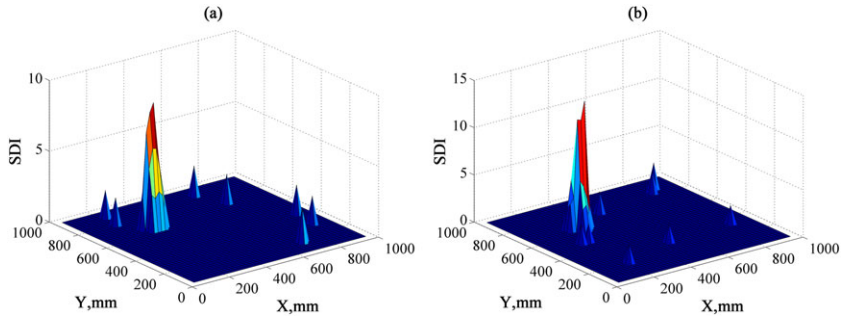

Figure 7. Standardized damage indices (SDIs) Z_{ij} for (a) the experimental and (b) simulated test cases after truncation according to the 95% confidence level.

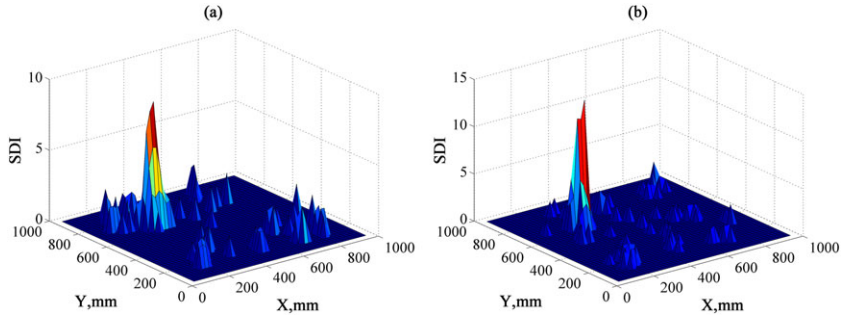

Figure 8. Standardized damage indices (SDIs) Z_{ij} for (a) the experimental and (b) simulated test cases after truncation according to the 90% confidence level.

$$R = \frac{\sum_{i,j=2}^{I-1} n\left(Z_{i,j} \geq 3\right)}{\sum_{i,j=2}^{I-1} 1} \times 100\% = \frac{\sum_{i,j=2}^{I-1} n\left(Z_{i,j} \geq 3\right)}{(I-2)\times(I-2)} \times 100\%, n\left(Z_{i,j} \geq 3\right) = \begin{cases} 1, \text{if } Z_{i,j} \geq 3 \\ 0, \text{if } Z_{i,j} < 3 \end{cases} \tag{7}$$

where $n(Z_{i,j} \geqslant 3)$ is related to those nodes, for which the standardized damage index value has passed the threshold value for the 99% confidence level for the presence of damage. Similarly, false-positive damage indication ratios are calculated for the other two confidence levels. Calculated false-positive damage indication ratios for the simulated test cases are summarized in Table 1. It must be noted that false-positive damage indication ratios are included in the table only for those simulated test cases where standardized damage indices at the predetermined damage location passed the standardized damage index threshold value for the corresponding confidence level. In general, the capability of the proposed damage detection algorithm is found to be dependent on both the introduced noise level and damage severity. As expected, the false-positive damage indication ratio R increases as the damage severity decreases and increases as the noise level is increased.

Standardized damage indices presented in Figures 9–13 illustrate the effectiveness of the proposed method when different numbers of measured mode shape datapoints are available for the damage detection. As seen from these figures, the method is able to correctly detect damage in all five simulated test cases and in four out of five times for the experimental test cases if the standardized damage index threshold value 3 for the 99% confidence level for the presence of damage is applied. However, its ability to accurately indicate the predetermined damage location and to illustrate the approximate shape of the damage gradually decreases as the sensor spacing increases. The method is still able to detect the damage when the lowest number of measurement points 11×11 is considered for the simulated test case, but it fails to accurately determine the predetermined location and size of

DOI: 10.1002/stc

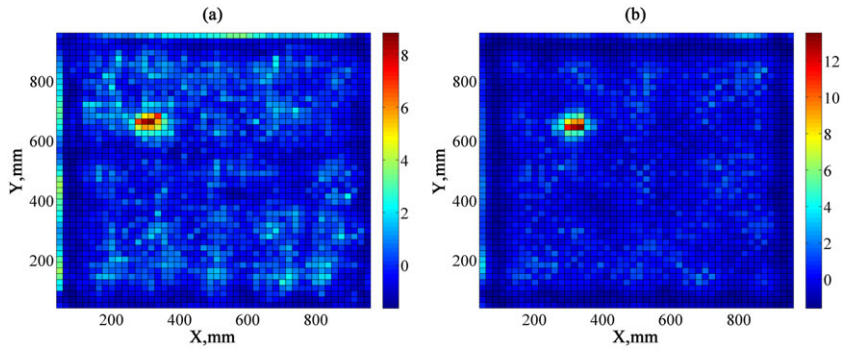

Figure 9. Standardized damage indices Z_{ij} for (a) the experimental and (b) simulated test cases using 51×51 mode shape datapoints.

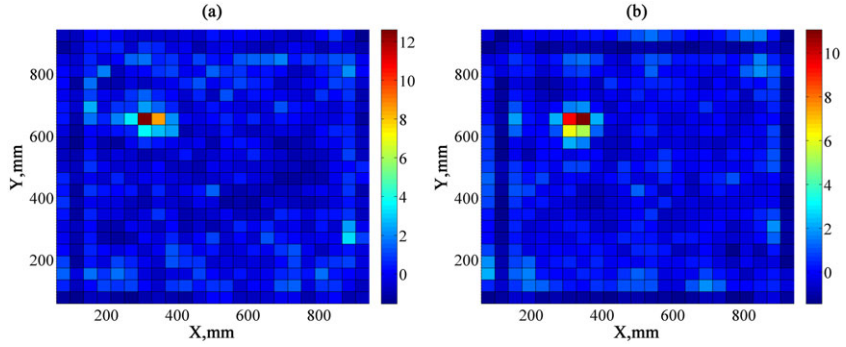

Figure 10. Standardized damage indices Z_{ij} for (a) the experimental and (b) simulated test cases using 26×26 mode shape datapoints.

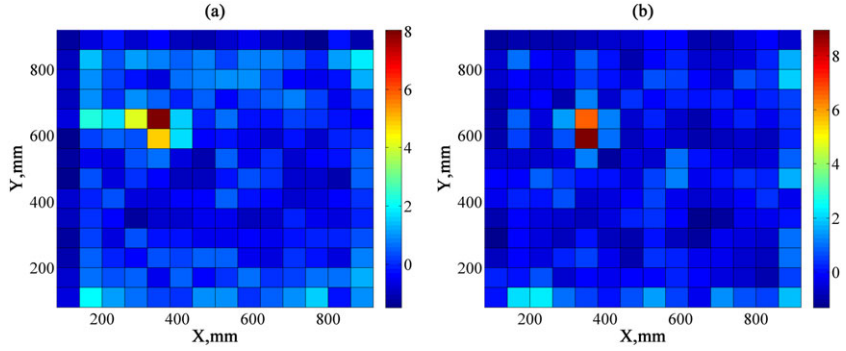

Figure 11. Standardized damage indices Z_{ij} for (a) the experimental and (b) simulated test cases using 17×17 mode shape datapoints.

the damage. The results show that robustness of the proposed damage detection algorithm under the limited measured datapoints is relatively good and the method can be applied for practical structural tests.

Standardized damage indices for the rectangular plate are given in Figures 14–18. Five different data sets, namely, original matrix of 51×21 calculated mode shape datapoints and the following reduced matrices of 26×11, 17×7, 13×6 and 11×5 datapoints, are considered for the damage detection. Figure 17 shows that the damage can reliably be detected by using just 13×6 measurement points. Similarly as for the square plate, the ability of the method to accurately determine the predetermined location and size of the damage gradually decreases as the sensor spacing

DOI: 10.1002/stc

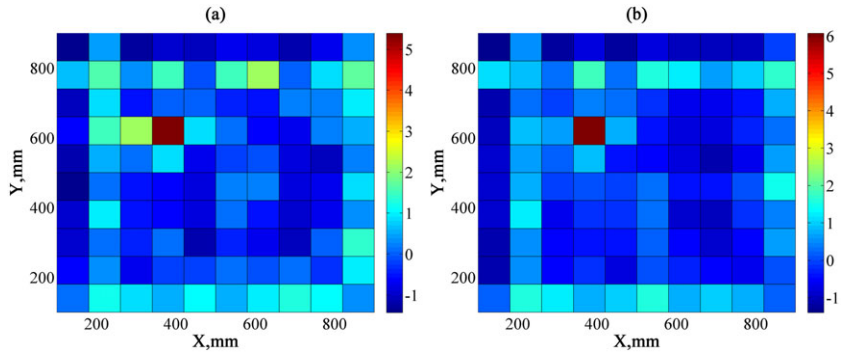

Figure 12. Standardized damage indices Z_{ij} for (a) the experimental and (b) simulated test cases using 13×13 mode shape datapoints.

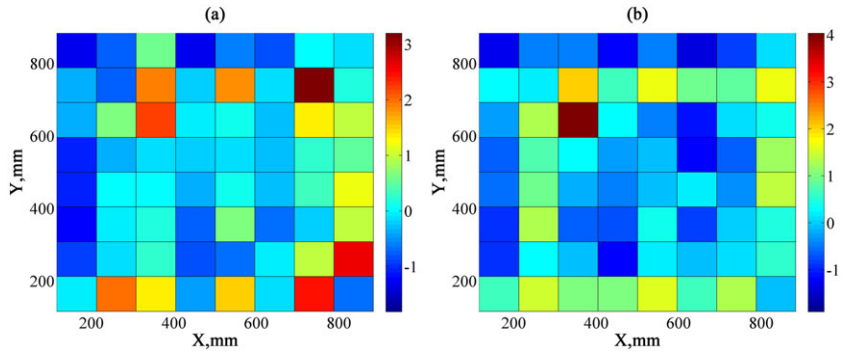

Figure 13. Standardized damage indices Z_{ij} for (a) the experimental and (b) simulated test cases using 11×11 mode shape datapoints.

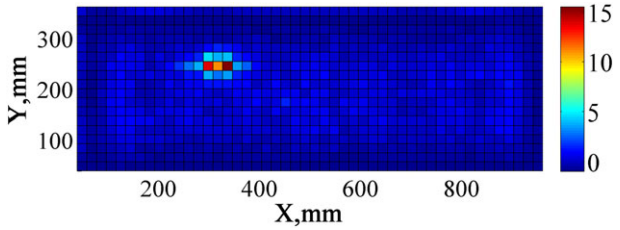

Figure 14. Standardized damage indices Z_{ij} for the rectangular plate using 51×21 mode shape datapoints.

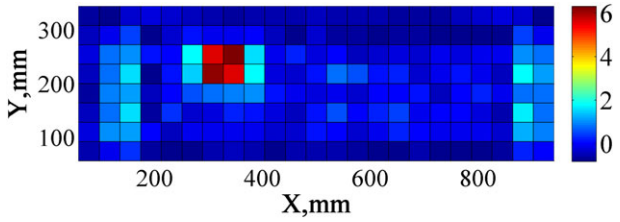

Figure 15. Standardized damage indices Z_{ij} for the rectangular plate using 26×11 mode shape datapoints.

increases. The results of this numerical experiment suggest that the proposed method can be successfully applied for damage detection in different aspect ratio plates under the limited measurement points.

DOI: 10.1002/stc

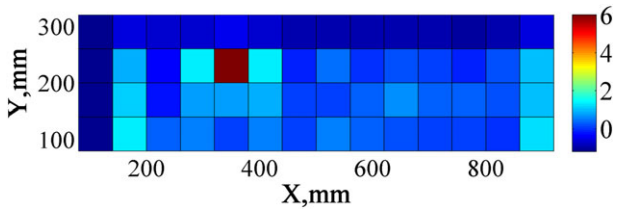

Figure 16. Standardized damage indices Z_{ij} for the rectangular plate using 17×7 mode shape datapoints.

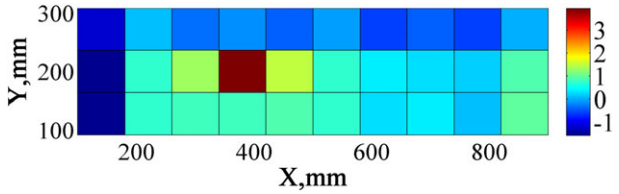

Figure 17. Standardized damage indices Z_{ij} for the rectangular plate using 13×6 mode shape datapoints.

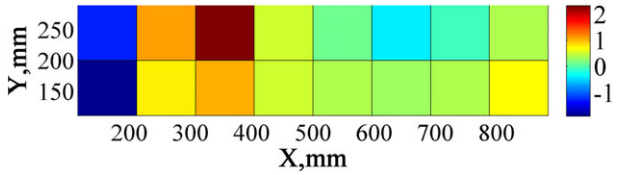

Figure 18. Standardized damage indices Z_{ij} for the rectangular plate using 11×5 mode shape datapoints.

6. CONCLUSIONS

In this paper, a numerical and experimental study on the applicability of mode shape curvature-based method for detection and localization of damage in plate-like structures has been presented. The advantage of the proposed method is that it requires mode shape information only from the damaged state of the structure. The damage index is defined as the absolute difference between the measured curvature of the damaged structure and the smoothed polynomial representing the healthy structure. Several sets of numerical simulations have been carried out to analyse the influence of damage severity, measurement noise and sensor spacing on the performance of the proposed damage detection method. The obtained results show that the proposed damage index provides reliable information about the location and size of the damage in case of the presence of medium severe damage, relatively accurate measurement data and relatively dense distribution of sensors. The last two drawbacks of the method can be overcome by using the latest scanning laser vibrometer systems that allow high-density transverse displacement measurements with a low degree of measurement noise ($\delta = 1 \times 10^{-2} \ldots 1 \times 10^{-3}$). In this case, the major drawback of the method is that the severity of damage has to be relatively high for successful damage detection. Robustness and effectiveness of the proposed damage detection method in combination with SLV system is demonstrated experimentally on an aluminium plate containing mill-cut damage. Validity of the proposed damage detection method is assessed by comparing the damage detection results of the experimental test case with the results obtained from the simulated test case. The obtained results suggest that the proposed method can be applicable not only for laboratory tests but also for practical structural applications.

ACKNOWLEDGEMENTS

The research leading to these results has received the funding from Latvia State Research Programme under grant agreement 'Innovative Materials and Smart Technologies for Environmental Safety, IMATEH'. The authors are also very grateful to the anonymous reviewers whose comments helped us to greatly improve the paper.

DOI: 10.1002/stc

REFERENCES

1. Doebling SW, Farrar CR, Prime MB, Shevith DW. Damage identification and health monitoring of structural and mechanical systems from changes in their vibration characteristics: literature review. *Los Alamos National Laboratory Report LA-13070-MS*, 1996.
2. Friswell MI. Damage identification using inverse methods. *Philosophical Transactions of the Royal Society A: Mathematical, Physical and Engineering Sciences* 2007; **365**:393–410. doi:10.1098/rsta.2006.1930.
3. Fan W, Qiao P. Vibration-based damage identification methods: a review and comparative study. *Structural Health Monitoring* 2011; **10**:83–111. doi:10.1177/1475921710365419.
4. Yuen MMF. A numerical study of the eigenparameters of a damaged cantilever. *Journal of Sound and Vibration* 1985; **103**:301–310. doi:10.1016/0022-460X(85)90423-7.
5. Pandey AK, Biswas M, Samman MM. Damage detection from changes in curvature mode shapes. *Journal of Sound and Vibration* 1991; **145**:321–332. doi:10.1016/0022-460X(91)90595-B.
6. Stubbs N, Kim JT. Damage localization in structures without baseline modal parameters. *American Institute of Aeronautics and Astronautics Journal* 1996; **34**:1644–1649.
7. Wahab A, Roeck G. Damage detection in bridges using modal curvatures: application to a real damage scenario. *Journal of Sound and Vibration* 1999; **226**:217–235. doi:10.1006/jsvi.1999.2295.
8. Maia NMM, Silva JMM, Almas EAM, Sampaio RPC. Damage detection in structures: from mode shape to frequency response function methods. *Mechanical Systems and Signal Processing* 2003; **17**:489–498. doi:10.1006/mssp.2002.1506.
9. Fan W, Qiao P. A 2-D continuous wavelet transform of mode shape data for damage detection of plate structures. *International Journal of Solids and Structures* 2009; **46**:4379–4395. doi:10.1016/j.ijsolstr.2009.08.022.
10. Rucevskis S, Wesolowski M, Chate A. Damage detection in laminated composite beam by using vibration data. *Journal of Vibroengineering* 2009; **11**:363–373.
11. Fu YZ, Lu ZR, Liu JK. Damage identification in plates using finite element model updating in time domain. *Journal of Sound and Vibration* 2013; **332**:7018–7032. doi:10.1016/j.jsv.2013.08.028.
12. Khiem NT, Tran HT. A procedure for multiple crack identification in beam-like structures from natural vibration mode. *Journal of Vibration Control* 2014; **20**:1417–1427. doi:10.1177/1077546312470478.
13. Perez MA, Gil L, Oller S. Impact damage identification in composite laminates using vibration testing. *Composite Structures* 2014; **108**:267–276. doi:10.1016/j.compstruct.2013.09.025.
14. Rucevskis S, Sumbatyan MA, Akishin P, Chate A. Tikhonov's regularization approach in mode shape curvature analysis applied to damage detection. *Mechanics Research Communications* 2015; **65**:9–16. doi:10.1016/j.mechrescom.2015.01.006.
15. Hamad WI, Owen JS, Hussein MFM. Modelling the degradation of vibration characteristics of reinforced concrete beams due to flexural damage. *Structural Control and Health Monitoring* 2015; **22**(6):939–967. doi:10.1002/stc.1726.
16. Hsu TY, Liao WI, Shiao SY. A pseudo local flexibility method for damage detection in hyperstatic beams. *Structural Control and Health Monitoring* 2015; **22**(4):682–693.
17. Shih HW, Thambiratnam DP, Chan THT. Damage detection in slab-on-girder bridges using vibration characteristics. *Structural Control and Health Monitoring* 2013; **20**(10):1271–1290. doi:10.1002/stc.1535.
18. Beskhyroun S, Wegner LD, Sparling BF. New methodology for the application of vibration-based damage detection techniques. *Structural Control and Health Monitoring* 2012; **19**(8):632–649. doi:10.1002/stc.456.
19. Ooijevaar TH, Warnet LL, Loendersloot R, Akkerman R, Tinga T. Impact damage identification in composite skin-stiffener structures based on modal curvatures. *Structural Control and Health Monitoring* 2016; **23**(2):198-217. doi:10.1002/stc.1754.
20. Alves V, Cury A, Roitman N, Magluta C, Cremona C. Novelty detection for SHM using raw acceleration measurements. *Structural Control and Health Monitoring* 2015; **22**(9):1193–1207. doi:10.1002/stc.1741.
21. Dworakowski Z, Kohut P, Gallina A, Holak K, Uhl T. Vision-based algorithms for damage detection and localization in structural health monitoring. *Structural Control and Health Monitoring* 2016; **23**(1):35-50. doi:10.1002/stc.1755.
22. Mosalam KM, Takhirov SM, Park S. Applications of laser scanning to structures in laboratory tests and field surveys. *Structural Control and Health Monitoring* 2014; **21**(1):115–134. doi:10.1002/stc.1565.
23. Dincal S, Stubbs N. Nondestructive damage detection in Euler–Bernoulli beams using nodal curvatures - part II: field measurements. *Structural Control and Health Monitoring* 2014; **21**(3):331–341. doi:10.1002/stc.1564.
24. Dincal S, Stubbs N. Nondestructive damage detection in Euler–Bernoulli beams using nodal curvatures – part I: theory and numerical verification. *Structural Control and Health Monitoring* 2014; **21**(3):303–316. doi:10.1002/stc.1562.
25. Ratcliffe CP, Bagaria WJ. A vibration technique for locating delamination in a composite beam. *American Institute of Aeronautics and Astronautics Journal* 1998; **36**:1074–1077.
26. Wu D, Law SS. Damage localization in plate structures from uniform load surface curvature. *Journal of Sound and Vibration* 2004; **276**:227–244. doi:10.1016/j.jsv.2003.07.040.
27. Qiao P, Lestari W, Shah MG, Wang J. Dynamics-based damage detection for composite laminated beams using contact and noncontact measurement systems. *Journal of Composite Materials* 2007; **41**:1217–1252. doi:10.1177/0021998306067306.
28. Gherlone M, Mattone M, Surace C, Tassoti A, Tessler A. Novel vibration-based methods for detecting delamination damage in composite plate and shell laminates. *Key Engineering Materials* 2005; **293-294**:289–296. doi:10.4028/www.scientific.net/KEM.293-294.289.
29. Matlab R2014a, http://se.mathworks.com
30. Bayissaa WL, Haritosa N, Thelandersson S. Vibration-based structural damage identification using wavelet transform. *Mechanical Systems and Signal Processing* 2008; **22**:1194–1215. doi:10.1016/j.ymssp.2007.11.001.